USC UNIVERSIDADE DE SANTIAGO DE COMPOSTELA
mat+i Grupo de Investigación en Ingeniería Matemática
SHARK-FV 2014 Conference
SHARING HIGHER-ORDER ADVANCED RESEARCH KNOW-HOW on FINITE VOLUME
www.math.univ-toulouse.fr/SHARK-FV
Ofir, Portugal
April 28 - May 2, 2014

A HIGH ORDER FINITE VOLUME/FINITE ELEMENT PROJECTION METHOD FOR LOW-MACH NUMBER FLOWS WITH TRANSPORT OF SPECIES

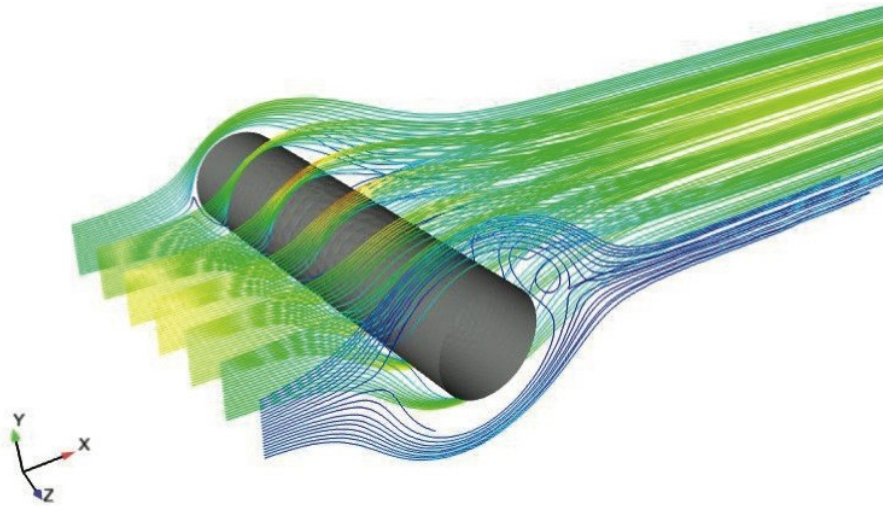

A. Bermúdez(*), S. Busto(*), M. Cobas (*), J.L. Ferrín(*), L. Saavedra(**) & M.E. Vázquez-Cendón(*)

(*) USC, (**) UPM

The Fundación Ciudad de la Energía is the leading public developer of CO_2 capture, transport and geological storage technologies in Spain.

- To develop technology to mitigate climate change through the development of CO2 capture, transport, and storage technologies.

- To conduct environmental studies related to energy, and to develop and apply environmental restoration techniques.
- To promote the training of researchers and technicians in the field of energy.

- To create, develop and then manage Ene. National Museum of Energy.
- To develop El Bierzo region socially and economically.

http://www.ciuden.es

Outline

- Low-Mach number equations
- Numerical discretization
  - A dual finite volume mesh
  - Finite volume discretization
  - Projection method
  - Coupling FVM and FEM
- Numerical results

Bermúdez, Ferrín, Saavedra, E. V-C **A projection hybrid finite volume/element method for low-Mach number flows,** *Journal of Computational Physics* Available online 25 September 2013

Low-Mach number equations

- Assumption: the Mach number M is sufficiently small so that the pressure p can be written as the sum of a spatially constant function $\overline{\pi}$ and a small perturbation π,

$$p(x,y,z,t) = \overline{\pi}(t) + \pi(x,y,z,t),\ \frac{\pi}{\overline{\pi}} = O(M^{-2}), \tag{1}$$

  - $\overline{\pi}(t)$ is a data
  - π is neglected in the state equation but it has to be retained in the momentum equation.

Low-Mach number equations

The compressible Navier-Stokes equations reduce to the mass conservation law, the momentum equation and the equation of state:

$$\frac{\partial \rho}{\partial t} + \operatorname{div}(\rho \mathbf{u}) = 0, \tag{2}$$

$$\frac{\partial \rho \mathbf{u}}{\partial t} + \underbrace{\frac{\partial F_1(\mathbf{u},\rho)}{\partial x} + \frac{\partial F_2(\mathbf{u},\rho)}{\partial y} + \frac{\partial F_3(\mathbf{u},\rho)}{\partial z}}_{\operatorname{div}(\mathbf{F}(\mathbf{u},\rho))} + \nabla \pi - \operatorname{div}\tau = \mathbf{f}(x,y,z,t), \tag{3}$$

$$\overline{\pi} = \rho R \theta. \tag{4}$$

- Density: $\rho = \rho(x,y,z,t)$
- Velocity vector: $\mathbf{u} = \mathbf{u}(x,y,z,t) = (u_1, u_2, u_3)'$
- Flux tensor, $\mathbf{F}$: $F_i(\mathbf{u},\rho) = \rho u_i \mathbf{u}$, $i = 1,2,3$
- The viscous part of the Cauchy stress tensor: τ
- Generic source term used in the analytical test problems: f
- The gas constant: $R = \mathcal{R}/\mathcal{M}$, the universal constant $\mathcal{R} = 8314\, J/(kmol\, K)$, the molecular mass $\mathcal{M}$ and the absolute temperature θ.

Low-Mach number equations

- From (2) and (4) we get the following divergence condition:

$$\operatorname{div}(\rho\mathbf{u}) = -\frac{\partial \rho}{\partial t} = -\frac{\partial}{\partial t}\left(\frac{\overline{\pi}}{R\theta}\right). \tag{5}$$

- Conservative variables: $\mathbf{w}(x,y,z,t) = \rho(x,y,z,t)\mathbf{u}(x,y,z,t)$

- Rewriting the flux in terms of $\mathbf{w}$,

$$\mathcal{F}_{\mathbf{i}}(\mathbf{w},\rho) = \frac{w_i}{\rho}\mathbf{w},\ i = 1,2,3.$$

- Now, the system of equations to be solved read

$$\frac{\partial \mathbf{w}}{\partial t} + \operatorname{div}(\mathcal{F}(\mathbf{w},\rho)) + \nabla\pi - \operatorname{div}(\tau) = \mathbf{f}(x,y,z,t), \tag{6}$$

$$\operatorname{div}\mathbf{w} = q, \tag{7}$$

where

$$q := -\frac{\partial}{\partial t}\left(\frac{\overline{\pi}}{R\theta}\right).$$

Numerical discretization

We start by considering $\mathbf{W^n}$, approximations of the conservative variables $\mathbf{w}(x, y, z, t^n)$ and π^n of the pressure $\pi(x, y, z, t^n)$, and define $\mathbf{W^{n+1}}$ and π^{n+1} from the following system of equations:

$$\frac{\widetilde{\mathbf{W}}^{\mathbf{n+1}} - \mathbf{W^n}}{\Delta t} + \operatorname{div}(\mathcal{F}(\mathbf{W^n}, \rho^n)) + \nabla \pi^n - \operatorname{div}(\tau^n) = \mathbf{f^n}, \tag{8}$$

$$\frac{\mathbf{W^{n+1}} - \widetilde{\mathbf{W}}^{\mathbf{n+1}}}{\Delta t} + \nabla(\pi^{n+1} - \pi^n) = 0, \tag{9}$$

$$\operatorname{div}\mathbf{W^{n+1}} = q^{n+1}. \tag{10}$$

Numerical discretization

Summarizing, the overall method consists of:

- *Transport-diffusion stage:* momentum equation (8) is solved by a FVM. The values $\widetilde{\mathbf{W}}^{\mathbf{n+1}}$ computed at this stage do not necessarily satisfy the divergence constraint at t^{n+1}.
- *Projection stage:* equations (9) and (10) are solved with a FEM to obtain the pressure correction $\delta^{n+1} := \pi^{n+1} - \pi^n$.
- *Post-projection stage:* the $\widetilde{\mathbf{W}}^{\mathbf{n+1}}$ computed at the first stage is updated by using δ^{n+1} in order to obtain another approximation $\mathbf{W}^{n+1}$ satisfying the divergence condition (10).

A dual finite volume mesh

- $\{N_i, \quad i = 1, M\}$ = barycentre of the "faces" of the tetrahedron.
- $\mathcal{K}_i$ = set of all the neighbors of N_i.
- $vol(C_i)$ = Volume of $\mathcal{C}_i$.
- $\Gamma_i = \partial V_i = \bigcup_{j \in \mathcal{K}_i} \Gamma_{ij}$, boundary of $\mathcal{C}_i$.

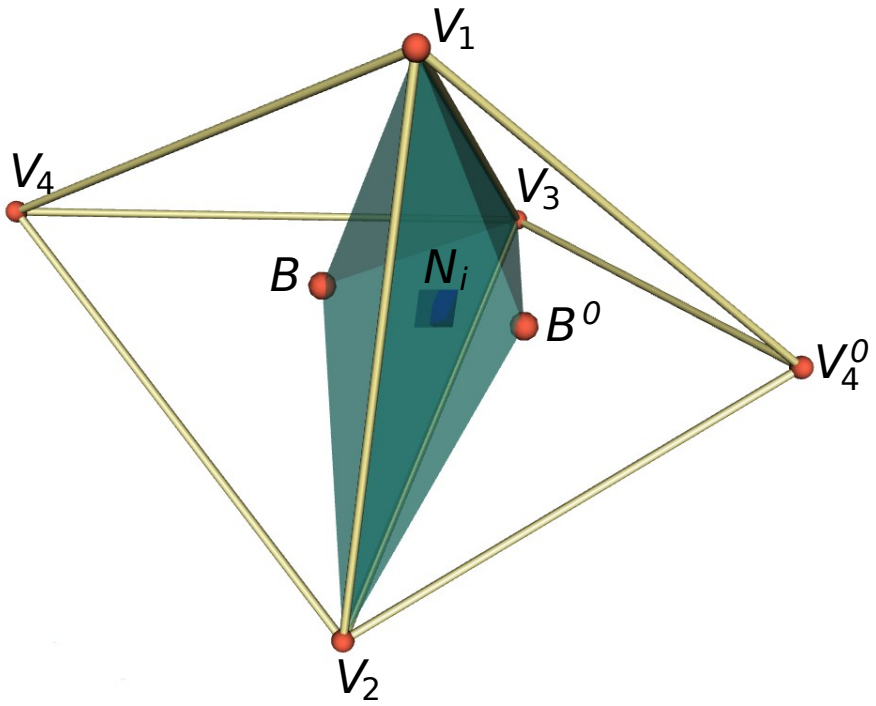

- $\mathbb{n}_j$ = outward normal to Γ_{ij}, $\mathbb{n}_j / \mathbb{n}_j = \mathbb{n}_j \|\mathbb{n}_j\|$,
- $S_i = \sum_{j 2 K_i} Area(\Gamma_{ij}) = \sum_{j 2 K_i} \|\mathbb{n}_j\|$=Area of Γ_i
- If N_i 2 Γ $\begin{cases} \Gamma_{if} = \Gamma_i \ T \ \otimes \\ \mathbb{n}_f = \text{outward normal} \end{cases}$

Finite volume discretization

- By integrating the momentum equation over the finite volume $\mathcal{C}_i$ and applying the Gauss' Theorem, we get

$$vol(C_i)\frac{\widetilde{\mathbf{W}}_i^{n+1} - \mathbf{W_i}^n}{\Delta t} + \int_{\Gamma_i} \mathcal{F}(\mathbf{W}^n, \rho^n)\tilde{\boldsymbol{\eta}}\, \mathrm{dS} = \int_{C_i} \left[-\nabla\pi^n + \mathrm{div}\tau^n + \mathbf{f}(x, y, z, t^n)\right] \mathrm{dV}, \quad (11)$$

- The integral of the normal flux:
  - Firstly, we split Γ_i into the cell interfaces Γ_{ij}:

$$\int_{\partial C_i} \mathcal{F}(\mathbf{W^n}, \rho^n)\tilde{\boldsymbol{\eta}}\, dS = \sum_{N_j \in \mathcal{K}_i} \int_{\Gamma_{ij}} \mathcal{F}(\mathbf{W^n}, \rho^n)\tilde{\boldsymbol{\eta}}_{\boldsymbol{ij}}\, \mathrm{dS}. \quad (12)$$

  - Then, in order to obtain a stable discretization, the integral on Γ_{ij} is approximated by an upwind scheme using a numerical flux function ϕ:

$$\int_{\Gamma_{ij}} \mathcal{F}(\mathbf{W^n}, \rho)\tilde{\boldsymbol{\eta}}_{\boldsymbol{ij}} \mathrm{dS} \approx \phi\left((\mathbf{W_i^n}, \rho_i^n), (\mathbf{W_j^n}, \rho_j^n), \boldsymbol{\eta}_{\boldsymbol{ij}}\right). \quad (13)$$

  - We will consider the Q-scheme of van Leer and the Rusanov scheme

Numerical flux: Q-scheme of van Leer

$$\begin{aligned}\phi((\mathbf{W_1},\rho_1),(\mathbf{W_2},\rho_2),\boldsymbol{\eta}) &= \frac{\mathcal{Z}(\mathbf{W_1},\rho_1,\boldsymbol{\eta})+\mathcal{Z}(\mathbf{W_2},\rho_2,\boldsymbol{\eta})}{2}\\ &- \frac{1}{2}\left|\mathcal{A}\left(\frac{\mathbf{W_1}+\mathbf{W_2}}{2},\frac{\rho_1+\rho_2}{2},\boldsymbol{\eta}\right)\right|(\mathbf{W_2}-\mathbf{W_1}),\end{aligned}$$

- $\mathcal{A}(\mathbf{W},\rho,\boldsymbol{\eta})$ Jacobian matrix of normal flux $\mathcal{Z}(\mathbf{W},\rho,\boldsymbol{\eta})$
- Eigenvalues $\lambda_1=\lambda_2=\frac{1}{\rho}\mathbf{W}\cdot\boldsymbol{\eta}=\mathbf{U}\cdot\boldsymbol{\eta}, \quad \lambda_3=\frac{2}{\rho}\mathbf{W}\cdot\boldsymbol{\eta}=2\mathbf{U}\cdot\boldsymbol{\eta}=2\lambda_1,$
- $\text{sign}(\lambda_1)$=$\text{sign}(\lambda_2)$=$\text{sign}(\lambda_3)$,
  - if $\text{sign}(\lambda_k)=1 \Longrightarrow |\mathcal{A}(\mathbf{W},\rho,\boldsymbol{\eta})|=\mathcal{A}(\mathbf{W},\rho,\boldsymbol{\eta})$
  - if $\text{sign}(\lambda_k)=-1 \Longrightarrow |\mathcal{A}(\mathbf{W},\rho,\boldsymbol{\eta})|=-\mathcal{A}(\mathbf{W},\rho,\boldsymbol{\eta}).$

Numerical flux: Rusanov scheme

$$\phi((\mathbf{W_1},\rho_1),(\mathbf{W_2},\rho_2),\boldsymbol{\eta})=\frac{\mathcal{Z}(\mathbf{W_1},\rho_1,\boldsymbol{\eta})+\mathcal{Z}(\mathbf{W_2},\rho_2,\boldsymbol{\eta})}{2}-\frac{1}{2}\alpha_{RS}\left(\mathbf{W_2}-\mathbf{W_1}\right),$$

$$\alpha_{RS}=\alpha_{RS}((\mathbf{W_1},\rho_1),(\mathbf{W_2},\rho_2),\boldsymbol{\eta}):=\max\left\{2\left|\mathbf{U_1}\cdot\boldsymbol{\eta}\right|,2\left|\mathbf{U_2}\cdot\boldsymbol{\eta}\right|\right\}.$$

Pressure explicit integral approximation

$$\int_{C_i} -\nabla \pi^n \, \mathrm{dV} = -\sum_{N_j \in \mathcal{K}_i} \int_{\Gamma_{ij}} \pi^n \, \widetilde{\boldsymbol{\eta}}_{\boldsymbol{ij}} \, \mathrm{dS}.$$

- The pressure is computed at the vertices of the original tetrahedral mesh, at the projection stage.
- Its value on face Γ_{ij} is approximated by the arithmetic mean of its values at the three vertices of face, namely, V_1, V_2 and the barycenter B,

$$\int_{\Gamma_{ij}} \pi \tilde{\eta}_{ij} dS = \tilde{\eta}_{ij} \frac{1}{3} \left(\pi(V_1) + \pi(V_2) + \pi(B)\right) Area(\Gamma_{ij})$$

with

$$\pi(B) = \tfrac{1}{4} \left(\pi(V_1) + \pi(V_2) + \pi(V_3) + \pi(V_4)\right)$$

- Finally the approximation of the integral reads

$$\int_{\Gamma_{ij}} \pi \tilde{\eta}_{ij} dS = \eta_{ij} \frac{1}{3} \left[\pi(V_1) + \pi(V_2) + \frac{1}{4} \left(\pi(V_1) + \pi(V_2) + \pi(V_3) + \pi(V_4)\right)\right]$$

Viscous term discretization

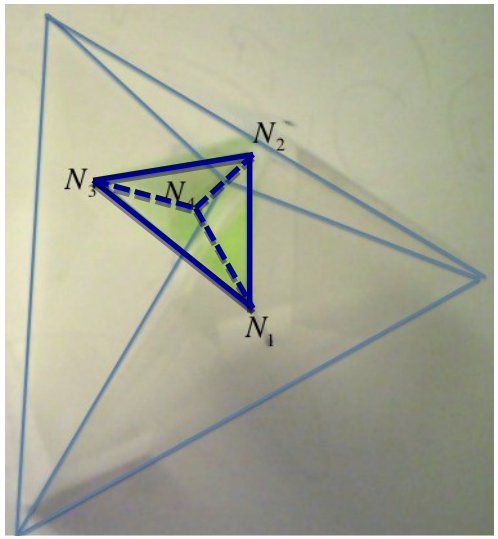

- Explicit discretization

$$\int_{C_i} \operatorname{div} \tau^n \, \mathrm{dV} \approx \sum_{j \in \mathcal{K}_i} \nu_{ij} \left(\nabla \mathbf{U^n} + (\nabla \mathbf{U^n})^T \right)_{ij} \boldsymbol{\eta_{ij}}$$

$$\begin{aligned} (\nabla \mathbf{U}^n)_{ij} &\approx \frac{1}{2} \left[\nabla \mathbf{U}^n{}_{T^i_{\Gamma_{ij}}} + \nabla \mathbf{U}^n{}_{T^j_{\Gamma_{ij}}} \right]. \\ (\nabla \mathbf{U}^n)_{ij} &\approx \nabla \mathbf{U}^n{}_{T_{\Gamma_{ij}}} \end{aligned}$$

- ν_{ij} is an approximation of the dynamic viscosity coefficient on face Γ_{ij}
- $\mathbf{U}^n_{T^i_{\Gamma_{ij}}}$, $\mathbf{U}^n_{T^j_{\Gamma_{ij}}}$ and $\mathbf{U}^n_{T_{\Gamma_{ij}}}$ denote linear interpolations of the velocity $\mathbf{U}$ in tetrahedra $T^i_{\Gamma_{ij}}$, $T^j_{\Gamma_{ij}}$ and $T_{\Gamma_{ij}}$, respectively
- As it is well known, for a linear scalar equation $w_t + \lambda w_x = \nu w_{xx}$, the stability condition for the upwind explicit scheme is

$$\Delta t \leq \frac{\Delta x}{\lambda + \frac{2\nu}{\Delta x}} = \frac{(\Delta x)^2}{\lambda \Delta x + 2\nu}.$$

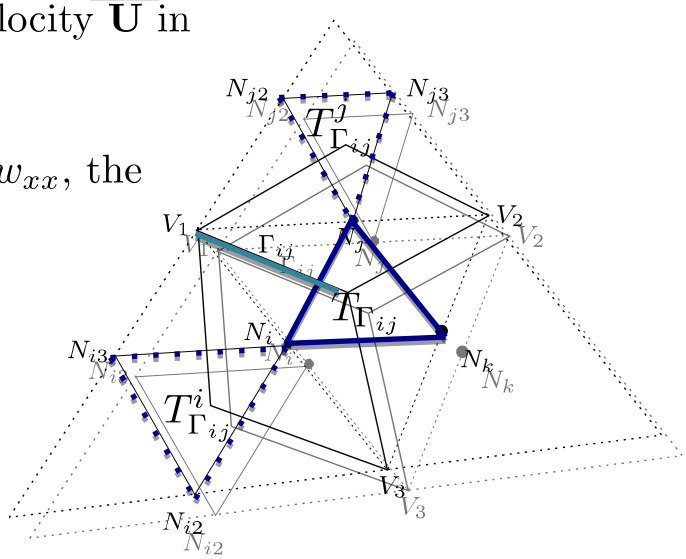

A new Kolgan-type scheme

$$\frac{\partial w}{\partial t}(x,t) + \frac{\partial f(w)}{\partial x}(x,t) = 0,$$

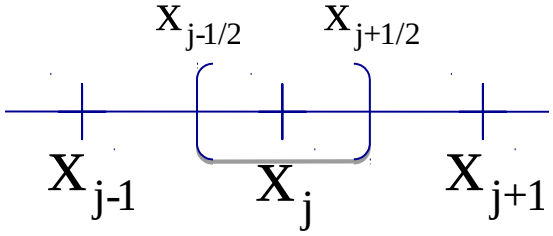

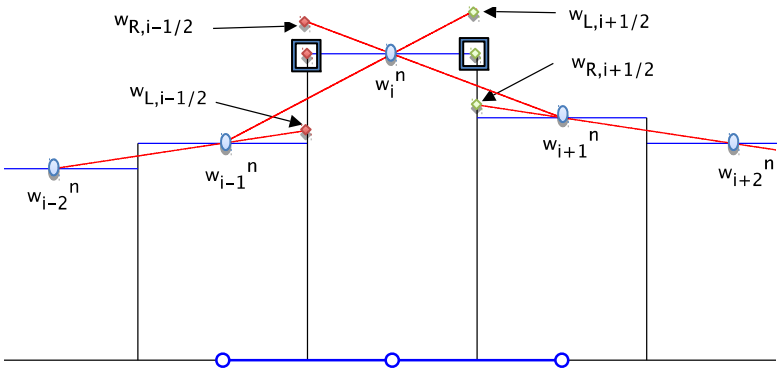

- New upwind x? order scheme

$$w_j^{n+1} = w_j^n - \frac{\Delta t}{\Delta x}\left(\phi(w_j^n, w_{j+1}^n, w_{L,j+1/2}^n, w_{R,j+1/2}^n) - \phi(w_{j-1}^n, w_j^n, w_{L,j-1/2}^n, w_{R,j-1/2}^n)\right)$$

- Numerical flux

$$\phi(U,V,U_L,V_R) = \frac{f(U)+f(V)}{2} - \frac{1}{2}\left|Q\left(U_L,V_R\right)\right|\left(V_R - U_L\right)$$

$$\mathbf{w}_{L,j-1/2} = \mathbf{w}_{j-1} + \frac{1}{2}\boldsymbol{\Delta}_{j-1}^{L*},\ \mathbf{w}_{R,j-1/2} = \mathbf{w}_j + \frac{1}{2}\boldsymbol{\Delta}_j^{R*}$$
$$\mathbf{w}_{L,j+1/2} = \mathbf{w}_j + \frac{1}{2}\boldsymbol{\Delta}_j^{L*},\ \mathbf{w}_{R,j+1/2} = \mathbf{w}_{j+1} + \frac{1}{2}\boldsymbol{\Delta}_{j+1}^{R*}$$

where $\boldsymbol{\Delta}_j^{L*}$, and $\boldsymbol{\Delta}_j^{R*}$ are the *left and right limited slopes* at the node x_j

$$\boldsymbol{\Delta}_j^{L*} = \begin{cases} \max\left[0, \min\left(\frac{\mathbf{w}_j - \mathbf{w}_{j-1}}{2}, \mathbf{w}_{j+1} - \mathbf{w}_j\right)\right] & \text{if } \mathbf{w}_{j+1} - \mathbf{w}_j > 0 \\ \min\left[0, \max\left(\frac{\mathbf{w}_j - \mathbf{w}_{j-1}}{2}, \mathbf{w}_{j+1} - \mathbf{w}_j\right)\right] & \text{if } \mathbf{w}_{j+1} - \mathbf{w}_j < 0 \end{cases}$$

$$\boldsymbol{\Delta}_j^{R*} = \begin{cases} \max\left[0, \min\left(-\frac{\mathbf{w}_{j+1} - \mathbf{w}_j}{2}, \mathbf{w}_{j-1} - \mathbf{w}_j\right)\right] & \text{if } \mathbf{w}_{j-1} - \mathbf{w}_j > 0 \\ \min\left[0, \max\left(-\frac{\mathbf{w}_{j+1} - \mathbf{w}_j}{2}, \mathbf{w}_{j-1} - \mathbf{w}_j\right)\right] & \text{if } \mathbf{w}_{j-1} - \mathbf{w}_j < 0 \end{cases}$$

E. V-C, L Cea. Analysis of a new Kolgan-type scheme motivated by the shallow water equations. *Applied Numerical Mathematics*, Volume 62, Issue 4, April 2012, Pages 489–506. 2012

Viscous term discretization

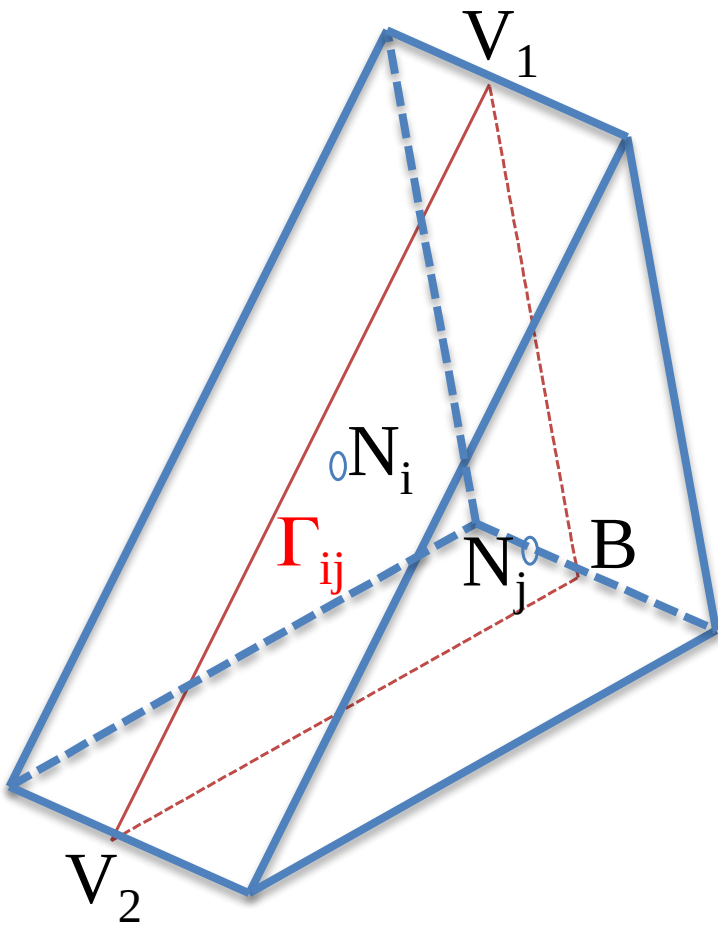

$\mathcal{V}_{ij}$

Diffusive flux D_{tot} decomposition on each face Γ_{ij}:

- *Orthogonal* diffusion $D_{\perp}^{ij}$
- *Non-orthogonal* diffusion $D_{\parallel}^{ij}$

- The approximation for each component of $\nabla \mathbf{U}$ on Γ_{ij} is given by

$$\begin{aligned}\left(\frac{\partial U_m}{\partial x_k}\right)_{ij} &\approx \frac{1}{\mathrm{vol}(\mathcal{V}_{ij})}\int_{\mathcal{V}_{ij}}\frac{\partial U_m}{\partial x_k}\,\mathrm{dV} = \frac{1}{\mathrm{vol}(\mathcal{V}_{ij})}\int_{\partial\mathcal{V}_{ij}} U_m n_k\,\mathrm{dS} \\ &= \frac{1}{\mathrm{vol}(\mathcal{V}_{ij})}\sum_{l=1}^{5} U_{ml}\,\mathrm{area}(\Gamma_l)n_k^l, \quad k=1,3 \qquad (14)\end{aligned}$$

$$\mathrm{vol}(\mathcal{V}_{ij}) = \|\boldsymbol{\eta}_{ij}\|\;|\,\widetilde{\boldsymbol{\eta}}_{\boldsymbol{ij}}\cdot\mathbf{N}_{ij}\,| = |\,\boldsymbol{\eta}_{ij}\cdot\mathbf{N}_{ij}\,|,\ \mathbf{N}_{ij}=N_i-N_j.$$

- Using (14), the approximation for the normal gradient component is:

$$\underbrace{\nu_{ij}\frac{\|\boldsymbol{\eta}_{ij}\|^2}{|\,\boldsymbol{\eta}_{ij}\cdot\mathbf{N}_{ij}\,|}[\mathbf{U}_j-\mathbf{U}_i]}_{D_{\perp}^{ij}} + \underbrace{\nu_{ij}\frac{1}{|\,\boldsymbol{\eta}_{ij}\cdot\mathbf{N}_{ij}\,|}\begin{pmatrix}\mathbf{U}(V_1) & \mathbf{U}(V_2) & \mathbf{U}(B)\end{pmatrix}\mathbf{r}_{\|_{ij}}}_{D_{\parallel}^{ij}},$$

$$\mathbf{r}_{\|_{ij}} = \langle(\boldsymbol{\eta}_{ij},\mathbf{V}_{B2},\mathbf{N}_{ij}),(\boldsymbol{\eta}_{ij},\mathbf{V}_{1B},\mathbf{N}_{ij}),(\boldsymbol{\eta}_{ij},\mathbf{V}_{21},\mathbf{N}_{ij})\rangle^T$$

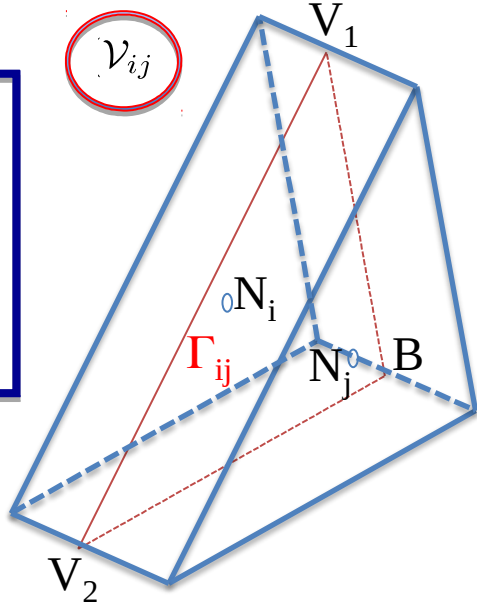

Viscous term discretization

- *Orthogonal* diffusion $D_{\perp}^{ij}$
  - In order to make implicit the main diagonal of the diffusion term, we introduce the component of the conservative variable $W_i = \rho_i U_i$ in $D_{\perp}^{ij}$:

$$D_{\perp}{}^{ij} = \nu_{ij} \frac{\|\boldsymbol{\eta}_{ij}\|^2}{|\,\boldsymbol{\eta}_{ij} \cdot \mathbf{N}_{ij}\,|} [\mathbf{U_j} - \mathbf{U_i}] = \nu_{ij} \frac{\|\boldsymbol{\eta}_{ij}\|^2}{|\,\boldsymbol{\eta}_{ij} \cdot \mathbf{N}_{ij}\,|} \left[\mathbf{U_j} - \frac{1}{\rho_i}\mathbf{W_i}\right], \quad (15)$$

  - Semi-implicit discretization

$$D_{\perp}{}^{ij} = \nu_{ij} \frac{\|\boldsymbol{\eta}_{ij}\|^2}{|\,\boldsymbol{\eta}_{ij} \cdot \mathbf{N}_{ij}\,|} \left[\mathbf{U_j^n} - \frac{1}{\rho_i}\mathbf{W_i^{n+1}}\right], \quad (16)$$

  * The coefficient in the i-th row of the main diagonal is

$$\frac{\Delta t}{vol(C_i)} \frac{1}{\rho_i^n} \sum_{j \in \mathcal{K}_i} \nu_{ij} \frac{\|\boldsymbol{\eta}_{ij}\|^2}{|\,\boldsymbol{\eta}_{ij} \cdot \mathbf{N}_{ij}\,|}. \quad (17)$$

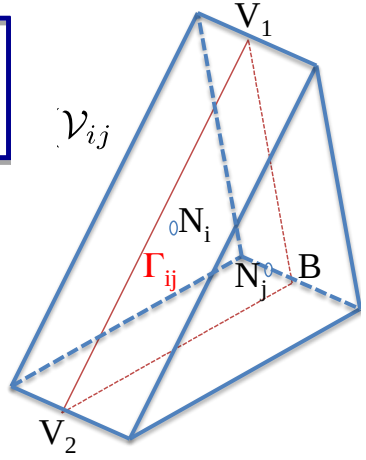

  - Explicit discretization

$$D_{\perp}{}^{ij} = \nu_{ij} \frac{\|\boldsymbol{\eta}_{ij}\|^2}{|\,\boldsymbol{\eta}_{ij} \cdot \mathbf{N}_{ij}\,|} \left[\mathbf{U_j^n} - \mathbf{U_i^n}\right], \quad (18)$$

Boundary conditions for the conservative variable

- *Transport-diffusion stage:* calculating $\widetilde{\mathbf{W}}^{n+1}$.
  - *Integral of the normal flux on a boundary face*

$$\int_{\Gamma_F} \mathcal{F}(\mathbf{W^n}, \rho) \cdot \widetilde{\boldsymbol{\eta}}_{\boldsymbol{F}} dS \approx \phi\left((\mathbf{W_F^n}, \rho_F^n), (\widehat{\mathbf{W}}_{\mathbf{F}}^{\mathbf{n}}, \widehat{\rho_F}^n), \boldsymbol{\eta_F}\right) = \mathcal{Z}(\mathbf{W_F^n}, \rho_F^n, \boldsymbol{\eta_F}).$$

  - *Integral of the pressure term on a boundary face*

$$\int_{\Gamma_F} \pi^n \widetilde{\boldsymbol{\eta}}_{\boldsymbol{F}} dS = \frac{1}{3}\left(\pi^n(V_{1F}) + \pi^n(V_{2F}) + \pi^n(V_{3F})\right) \mathrm{area}(\Gamma_F)\, \widetilde{\boldsymbol{\eta}}_{\boldsymbol{F}}.$$

  - **Dirichlet boundary conditions**
    - *Inviscid fluids.* $\mathbf{w} \cdot \widetilde{\boldsymbol{\eta}}_{\partial\Omega} = g$

$$\widetilde{\mathbf{W}_F}^{n+1} \leftarrow \widetilde{\mathbf{W}_F}^{n+1} - \widetilde{\mathbf{W}_F}^{n+1} \widetilde{\boldsymbol{\eta}}_{\boldsymbol{F}}\, \widetilde{\boldsymbol{\eta}}_{\boldsymbol{F}} + g(N_F, t^{n+1}, \widetilde{\boldsymbol{\eta}}_{\boldsymbol{F}}) \widetilde{\boldsymbol{\eta}}_{\boldsymbol{F}}.$$

    - *Viscous fluids.* The conservative variable $\mathbf{w}$ is imposed at the boundary.
  - **Neumann boundary conditions** The computation of $\widetilde{\mathbf{W}_F}^{n+1}$ takes into account the inflow/outflow boundary condition.
- *Post-projection stage:* calculating $\mathbf{W}^{n+1}$. After updating the conservative variables, depending on the existence of viscous terms it may be necessary to impose some boundary conditions.

Projection method

We have adapted the incremental projection method used in Guermond *et al* (2006).

$$\left.\begin{aligned} \frac{\widetilde{W}^{n+1}-W^n}{\Delta t}+\operatorname{div}(\mathcal{F}((\rho U)^n,\rho^n))+\nabla\pi^n-\operatorname{div}\tau^n=f^n\,[Output:\widetilde{W}^{n+1}\,Transport\text{-}diffusion\ stage] \\ \frac{W^{n+1}-\widetilde{W}^{n+1}}{\Delta t}+\nabla(\pi^{n+1}-\pi^n)=0\,[Output:\pi^{n+1}-\pi^n\,Projection\ stage] \\ \operatorname{div}(W^{n+1})=q^{n+1}[Projection\ stage] \end{aligned}\right\}(*)$$

- We solve (*) and obtain $\pi^{n+1}-\pi^n$ using a standard finite element method.
- Multiplying this equation by ∇z and integrating over Ω we obtain the following variational formulation:

$$\int_\Omega \nabla(\pi^{n+1}-\pi^n)\cdot\nabla z=\frac{1}{\Delta t}\int_\Omega \widetilde{\mathbf{W}}^{\mathbf{n+1}}\cdot\nabla z-\frac{1}{\Delta t}\int_\Omega \mathbf{W}^{\mathbf{n+1}}\cdot\nabla z\quad\forall z\in V_0,$$

where $V_0:=\left\{z\in H^1(\Omega):\int_\Omega z=0\right\}$.

- Using the divergence condition and the Green formula, $\int_\Omega W^{n+1}\cdot\nabla z$ read:

$$\int_\Omega W^{n+1}\cdot\nabla z=\int_{\partial\Omega}\underbrace{W^{n+1}\cdot n\,z}_{g^{n+1}\,z}-\int_\Omega\underbrace{\operatorname{div}(W^{n+1})\,z}_{q^{n+1}\,z}$$

Projection method

- Replacing the previous expression in the variational formulation and introducing the variable $\delta^{n+1} := \pi^{n+1} - \pi^n$, to obtain π^{n+1} we need to solve the weak problem:

Find $\delta^{n+1} \in V_0$ *verifying*

$$\int_\Omega \nabla\delta^{n+1}\cdot\nabla z = \frac{1}{\Delta t}\int_\Omega \widetilde{\mathbf{W}}^{\mathbf{n+1}}\cdot\nabla z + \frac{1}{\Delta t}\int_\Omega q^{n+1}z - \frac{1}{\Delta t}\int_{\partial\Omega} g^{n+1}z$$

- This weak problem can bee seen as corresponding to the following Laplace problem with Neumann conditions

$$\Delta\delta^{n+1} = \frac{1}{\Delta t}(\,\mathrm{div}(\widetilde{\mathbf{W}}^{\mathbf{n+1}}) - q^{n+1}) \text{ in } \Omega,$$
$$\frac{\partial\delta^{n+1}}{\partial\mathbf{n}} = \frac{1}{\Delta t}(\widetilde{\mathbf{W}}^{\mathbf{n+1}}\cdot\mathbf{n} - g^{n+1}) \text{ in } \Gamma.$$

Post-projection stage

- Finally, with δ^{n+1}, the value of $\mathbf{W}^{\mathbf{n+1}}$ at each finite volume is obtained from (9) at the *post-projection stage:*

$$\mathbf{W}_\mathbf{i}^{\mathbf{n+1}} = \widetilde{\mathbf{W}}_\mathbf{i}^{\mathbf{n+1}} - \Delta t\nabla\delta_i^{n+1},$$

where $\nabla\delta_i^{n+1}$ denotes the arithmetic mean of $\nabla\delta^{n+1}$ at the two tetrahedra having N_i as barycenter of one common face.

Coupling between the *Transport-diffusion stage* and *Projection stage*

- *Projection stage*: it is necessary to compute the integral $\int_T \widetilde{\mathbf{W}} \cdot \nabla p_i^T$, where T is an element of the finite element mesh and p_i^T a basis function in T. We assume $\widetilde{\mathbf{W}}$ is constant per finite element ($\widetilde{\mathbf{W}}_T$)
- *Transport-diffusion stage*: the values of $\widetilde{\mathbf{W}}$ are constant per finite volume.
- The difficulty of the coupling lies in the computation of $\widetilde{\mathbf{W}}_T$.
- The solutions:

X **Unstable coupling:** $\widetilde{\mathbf{W}}_T$ is computed via the vertices of the tetrahedron

$$\widetilde{\mathbf{W}}(\text{Nodes FV mesh}) \rightarrow \widetilde{\mathbf{W}}(\text{Vertices FE mesh}) \rightarrow \widetilde{\mathbf{W}}(\text{tetrahedron})$$

$$\widetilde{\mathbf{W}}_T = \frac{1}{4}\left(\widetilde{\mathbf{W}}(V_1) + \widetilde{\mathbf{W}}(V_2) + \widetilde{\mathbf{W}}(V_3) + \widetilde{\mathbf{W}}(V_4)\right),$$

√ **Stable coupling:** $\widetilde{\mathbf{W}}_T$ is computed via the nodes of the tetrahedron

$$\widetilde{\mathbf{W}}(\text{Nodes FV mesh}) \rightarrow \widetilde{\mathbf{W}}(\text{tetrahedron}),$$

$$\widetilde{\mathbf{W}}_T = \frac{1}{4}\left(\widetilde{\mathbf{W}}(N_1) + \widetilde{\mathbf{W}}(N_2) + \widetilde{\mathbf{W}}(N_3) + \widetilde{\mathbf{W}}(N_4)\right).$$

Numerical Results

1. Academic test for Euler equations

- The flow is defined by

$$\mathbf{w}(x,y,z,t) = \rho(x,y,z,t)\mathbf{u}(x,y,z,t) = e^{xt}(e^x, y^2+1, z^2)^T,$$
$$\pi(x,y,z,t) = \frac{1}{2}e^t(x^2+y^2+z^2),$$

The corresponding source term f is:

$$\mathbf{f}(x,y,z,t) := \begin{pmatrix} xe^{x(t+1)} + (2+t)e^{x(t+2)} + 2(y+z)e^{x(t+1)} + 2ze^{x(t+1)} + xe^t \\ xe^{xt} + ye^t + (t+1)(y^2+1)e^{x(t+1)} + 2(y^2+1)(2y+z)e^{xt} \\ xz^2e^{xt} + z^2(t+1)e^{x(t+1)} + 2yz^2e^{xt} + 4z^3e^{xt} + ze^t \end{pmatrix}$$

- Features of the meshes

Mesh	$N = 1/h$	Elements (nel)	Vertices (M)	Nodes	V_h^m (m^3)	V_h^M (m^3)
$M1$	4	384	125	864	6.51E-04	1.30E-03
$M2$	8	3072	729	6528	8.14E-05	1.63E-04
$M3$	16	24576	4913	50688	1.02E-05	2.03E-05

- To check the order of the error we compute the norms

$$E(\mathbf{w}) = \|\mathbf{w} - \mathbf{w}_h\|_{l^2(L^2(\Omega)^3)}, \quad E(\pi) = \|\pi - \pi_h\|_{l^2(L^2(\Omega))},$$

1. Academic test for Euler equations

$$\mu^n = \max_{i=1,nod} \Delta t 2 \|\mathbf{U}_i^n\| \frac{S_i}{vol(C_i)},$$

$$\Delta t^n = \min_{i=1,nod} \frac{\mu\, vol(C_i)}{2\|\mathbf{U}_i^n\| S_i}.$$

1. Academic test for Euler equations

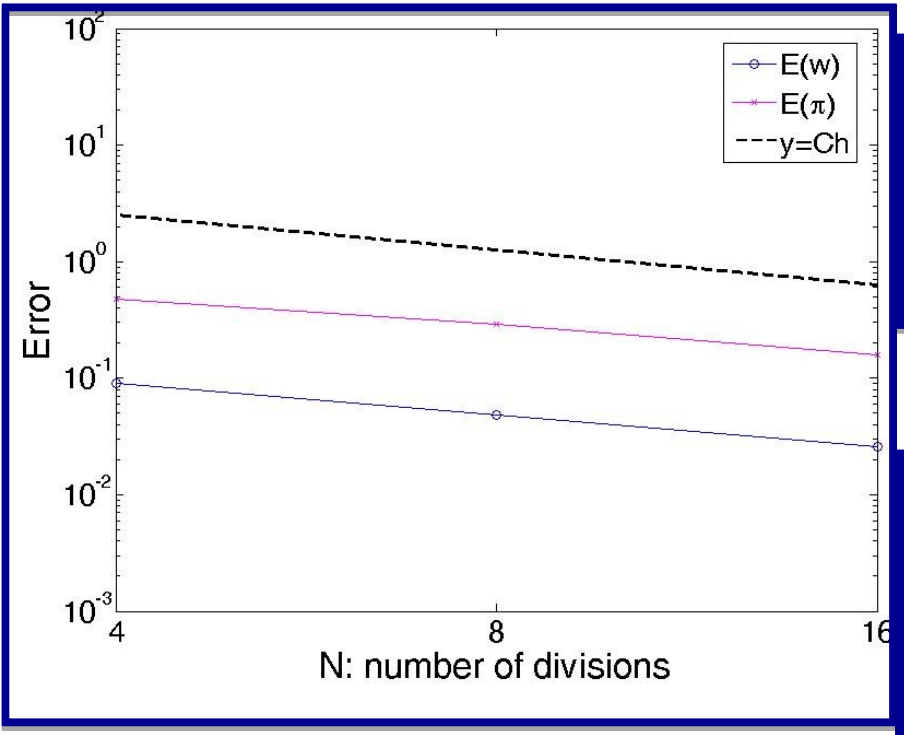

Errors $E(\mathbf{w})_{M_k} = \|\mathbf{w} - \mathbf{w}_{M_k}\|_{l^2(L^2(\Omega))}$, $k = 1, 2, 3$.

CFL	$E(\mathbf{w})_{M_1}$	$E(\mathbf{w})_{M_2}$	$E(\mathbf{w})_{M_3}$
6	2.90E−01	1.21E−01	4.96E−02
4	6.77E−03	3.30E−03	1.63E−03
3	9.03E−02	4.85E−02	2.59E−02
2	3.38E−03	1.65E−03	8.14E−04
1.5	9.04E−02	4.85E−02	2.59E−02
1	1.69E−03	8.26E−04	4.07E−04
0.75	9.05E−02	4.86E−02	2.59E−02

Ratios of spatial errors $E(\mathbf{w})_{M_1}/E(\mathbf{w})_{M_2}$ and $E(\mathbf{w})_{M_2}/E(\mathbf{w})_{M_3}$.

CFL	$E(\mathbf{w})_{M_1}/E(\mathbf{w})_{M_2}$	$E(\mathbf{w})_{M2}/E(\mathbf{w})_{M_3}$
6	2.4012	2.4367
4	1.8610	1.8745
3	1.8618	1.8749
2	1.8626	1.8752
1.5	1.8631	1.8754
1	1.8635	1.8756
0.75	1.8638	1.8638

2. Euler flow around a sphere

This problem was discussed by Landau and Lifshitz

- A sphere of radius $R = 1$ centered at the origin is surrounded by the computational domain of the flow, consisting in a cube of dimensions $\Omega = [-4, 4]^3$.
- The parameters of the flow

$$M_\infty = 10^{-2}, \quad \gamma = 1.4, \quad \rho_\infty = 1, \quad \pi_\infty = \frac{1}{\gamma}, \quad c_\infty = 1, \quad u_\infty = M_\infty c_\infty = 10^{-2}$$

- The analytic solution, expressed in cartesian coordinates

$$\begin{aligned} \mathbf{u}(x,y,z,t) &= \mathbf{u}_\infty + \frac{1}{2}\left(\frac{R}{r(x,y,z)}\right)^3 \left[-3\frac{\mathbf{r}(x,y,z)}{r^2(x,y,z)}\mathbf{u}_\infty \cdot \mathbf{r}(x,y,z) + \mathbf{u}_\infty\right], \\ \pi(x,y,z,t) &= \pi_\infty + \rho_0\left(\frac{1}{2}u_\infty^2 - \frac{1}{2}\|\mathbf{u}(x,y,z)\|^2\right). \end{aligned}$$

$\mathbf{r}$ is the position vector, $r = \|\mathbf{r}\|$ and $\mathbf{u}_\infty = u_\infty \mathbf{e_1}$.

2. Euler flow around a sphere

Boundary	Surface	Type (*Transport-diffusion stage*)	Condition
Γ_i, inlet flow	$x = -4$	Dirichlet	$w \cdot \mathbf{n} = g$
Γ_w, wall	$r = 1$, $y = -4$, $y = 4$, $z = -4$ y $z = 4$	Dirichlet	$w \cdot \mathbf{n} = g$
Γ_o, outlet flow	$x = 4$	Neumann	$\frac{\partial w}{\partial \mathbf{n}} = 0$

Table 3: Boundary conditions for the flow around a sphere

- The algorithm is started with the following values for velocity and pressure:

$$\mathbf{u}(x,y,z)_0 = \begin{cases} u_\infty \mathbf{e_1} & \text{if} \quad (x,y,z) \in \Gamma_i \\ 0 & \text{in other case} \end{cases}$$

$$\pi(x,y,z)_0 = \begin{cases} p_\infty & \text{if} \quad (x,y,z) \in \Gamma_i \\ 0 & \text{in other case} \end{cases}$$

The mesh M employed

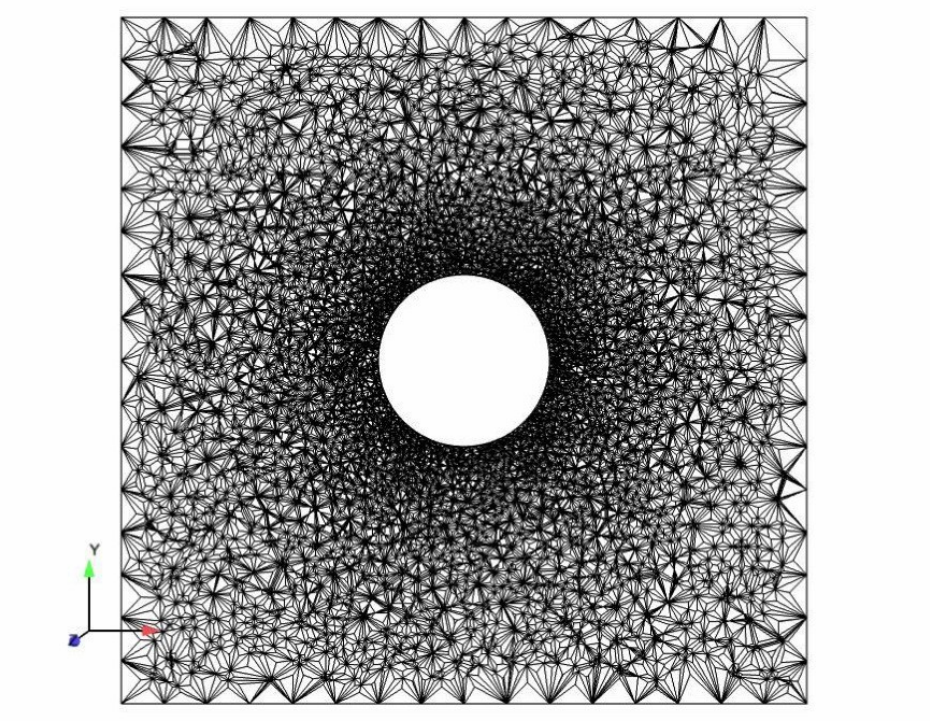

Finite volume mesh section in z = 0

- 318684 tetrahedra,
- 55022 vertices
- 641149 finite volumes

Steady state

$$\Delta \mathbf{W}_M^{out}/\Delta t := \frac{1}{\Delta t}\|\mathbf{W}_M^{out} - \mathbf{W}_M^{out-1}\|_{L^2(\Omega)^3},$$

Δt	time iterations	μ^{out}	CPU time	$\Delta \mathbf{W}_M^{out}/\Delta t$	$E(\mathbf{w})_M$	$E(\pi)_M$
0.4	25	4.12	00:02:21	5.37E-05	7.46E-4	1.22E-5
0.3	34	3.09	00:03:03	4.33E-05	7.16E-4	1.17E-5
0.2	50	2.06	00:04:06	3.78E-05	6.93E-4	1.14E-5
0.1	100	1.03	00:07:42	3.33E-05	6.79E-4	1.12E-5
0.05	200	0.51	00:14:48	3.19E-05	6.75E-4	1.11E-5

- $\Delta t = 0.45$ the numerical method is unstable
- The computer code was written in Fortran 90 and ran on a node of a cluster with a processor Intel Xeon CPU X5570@2.93GHz

2. Euler flow around a sphere

Streamlines and pressure contours on the sphere

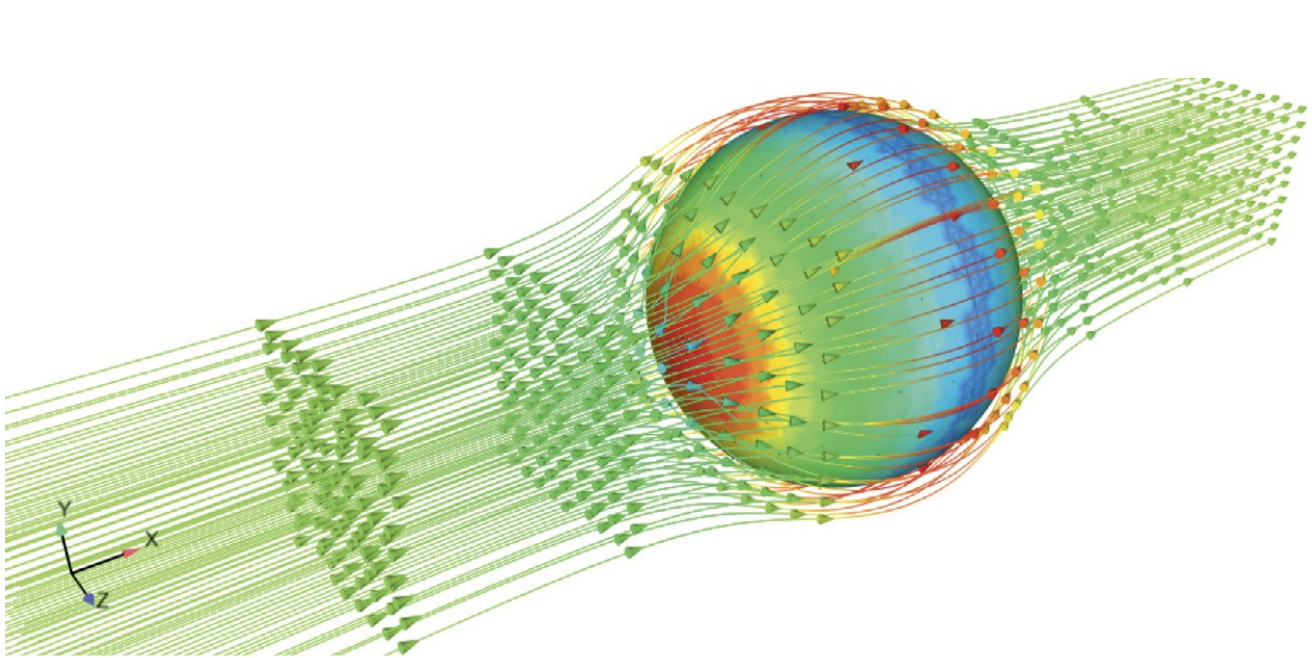

Δt=0.2at t=10

2. Euler flow around a sphere

Z=0 Δt=0.2at t=10

w

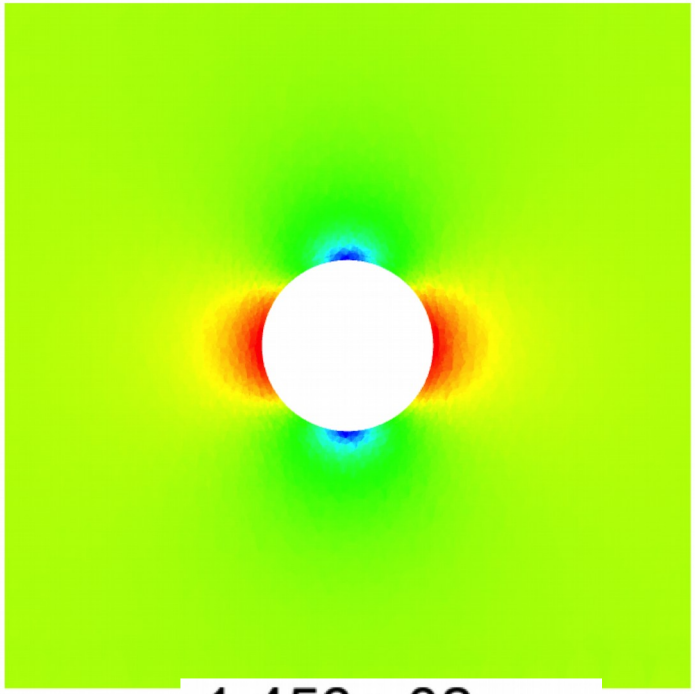

1.456e-02
1.096e-02
7.350e-03
3.743e-03
1.354e-04

π

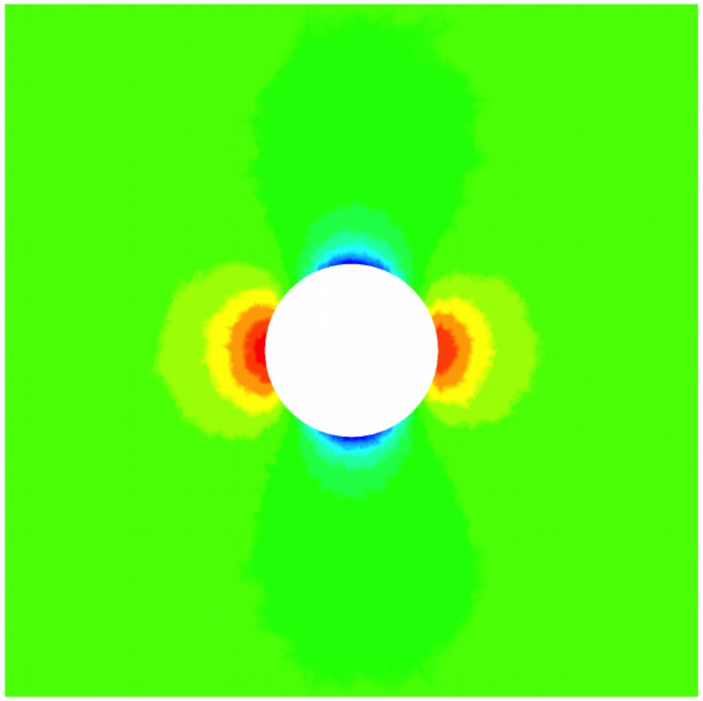

7.143e-01
7.143e-01
7.143e-01
7.142e-01
7.142e-01

Numerical Results

Academic test for Navier-Stokes equations

- Exact solution:

$$\begin{aligned}&\mathbf{w}(x,y,z,t) = (\sin(\pi t y), -\cos(\pi t z), e^{-\pi x t})^T,\\ &\pi(x,y,z,t) = \cos(\pi t(x+y+z))\\ &\rho(x,y,z,t) = 1\end{aligned}$$

The corresponding source term f is:

$$\mathbf{f}(x,y,z,t) := \begin{pmatrix} \pi y\cos(\pi t y) - \pi t\cos(\pi t z)\cos(\pi t y) - \pi t\sin(\pi t(x+y+z)) + \nu\pi^2 t^2\sin(\pi t y)\\ \pi z\sin(\pi t z) + \pi t\sin(\pi t z)e^{-\pi t x} - \pi t\sin(\pi t(x+y+z)) - \nu\pi^2 t^2\cos(\pi t z)\\ -\pi x e^{-\pi t x} - \pi t\sin(\pi t y)e^{-\pi t x} - \pi t\sin(\pi t(x+y+z)) - \nu\pi^2 t^2\cos(\pi t x)\end{pmatrix}.$$

- Features of the meshes

Mesh	$N = 1/h$	Elements (nel)	Vertices (M)	Nodes	V_h^m (m^3)	V_h^M (m^3)
$M1$	4	384	125	864	6.51E-04	1.30E-03
$M2$	8	3072	729	6528	8.14E-05	1.63E-04
$M3$	16	24576	4913	50688	1.02E-05	2.03E-05

- To check the order of the error we compute the norms

$$E(\mathbf{w}) = \|\mathbf{w} - \mathbf{w}_h\|_{l^2(L^2(\Omega)^3)}, \quad E(\pi) = \|\pi - \pi_h\|_{l^2(L^2(\Omega))},$$

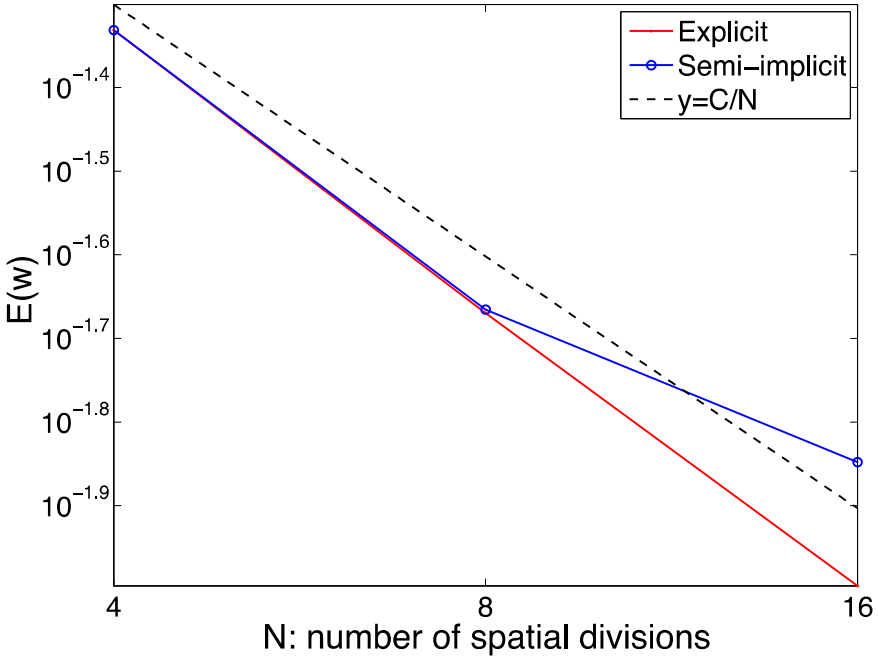

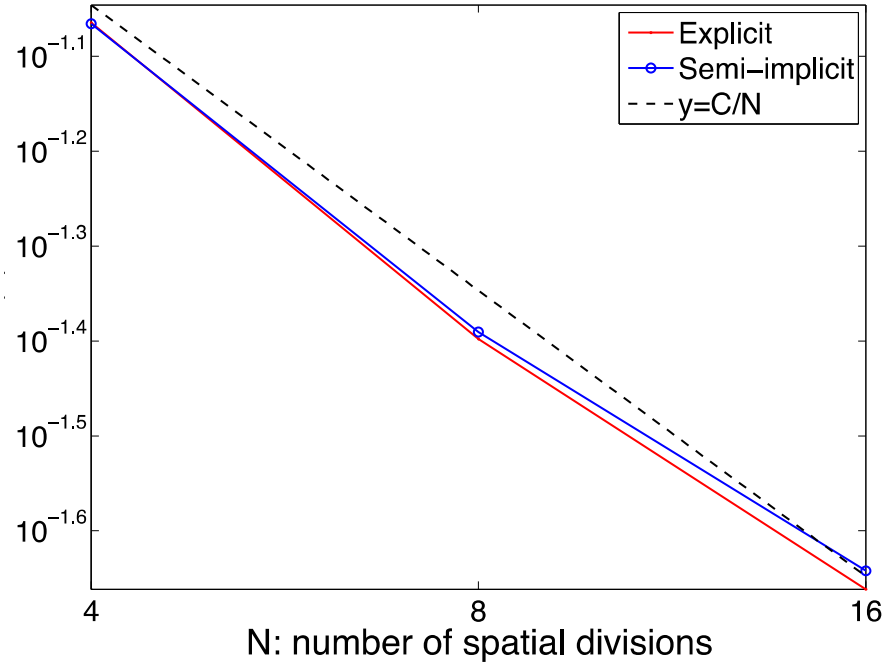

Errors E(w) (left) and E(π) (right) obtained setting the time step to t =4.88E-4

The explicit discretization

Δt	$E(\mathbf{w})_{M1}/E(\mathbf{w})_{M2}$	$E(\mathbf{w})_{M2}/E(\mathbf{w})_{M3}$
1.95E-03	2.18E+00	2.12E+00
9.77E-04	2.18E+00	2.12E+00
4.88E-04	2.18E+00	2.12E+00

Table 7: Ratios of spatial errors $E(\mathbf{w})_{M1}/E(\mathbf{w})_{M2}$ and $E(\mathbf{w})_{M2}/E(\mathbf{w})_{M3}$.

Δt	$E(\pi)_{M_1}$	$E(\pi)_{M_2}$	$E(\pi)_{M_3}$
1.95E-03	8.55E-02	3.92E-02	2.11E-02
9.77E-04	8.60E-02	3.97E-02	2.15E-02
4.88E-04	8.62E-02	4.00E-02	2.18E-02

Table 8: Errors $E(\pi)_{M_k} = \|\pi - \pi_{M_k}\|_{l^2(L^2(\Omega))}$, $k = 1, 2, 3$.

Δt	$E(\pi)_{M1}/E(\pi)_{M2}$	$E(\pi)_{M2}/E(\pi)_{M3}$
1.95E-03	2.18E+00	1.85E+00
9.77E-04	2.16E+00	1.85E+00
4.88E-04	2.15E+00	1.84E+00

Table 9: Ratios of spatial errors $E(\pi)_{M1}/E(\pi)_{M2}$ and $E(\pi)_{M2}/E(\pi)_{M3}$.

The semi-implicit discretization

Δt	$E(\mathbf{w})_{M_1}$	$E(\mathbf{w})_{M_2}$	$E(\mathbf{w})_{M_3}$
1.95E-03	4.67E-02	2.33E-02	3.56E-02
9.77E-04	4.66E-02	2.20E-02	2.11E-02
4.88E-04	4.66E-02	2.16E-02	1.42E-02

Table 10: Errors $E(\mathbf{w})_{M_k} = \|\mathbf{w} - \mathbf{w}_{M_k}\|_{l^2(L^2(\Omega))}$, $k = 1, 2, 3$.

Δt	$E(\mathbf{w})_{M1}/E(\mathbf{w})_{M2}$	$E(\mathbf{w})_{M2}/E(\mathbf{w})_{M3}$
1.95E-03	2.01E+00	6.54E-01
9.77E-04	2.12E+00	1.04E+00
4.88E-04	2.16E+00	1.52E+00

Table 11: Ratios of spatial errors $E(\mathbf{w})_{M1}/E(\mathbf{w})_{M2}$ and $E(\mathbf{w})_{M2}/E(\mathbf{w})_{M3}$.

The semi-implicit discretization

Δt	$E(\pi)_{M_1}$	$E(\pi)_{M_2}$	$E(\pi)_{M_3}$
1.95E-03	8.51E-02	5.32E-02	3.56E-02
9.77E-04	8.56E-02	4.32E-02	7.75E-02
4.88E-04	8.60E-02	4.07E-02	4.28E-02

Table 12: Errors $E(\pi)_{M_k} = \|\pi - \pi_{M_k}\|_{l^2(L^2(\Omega))}$, $k = 1, 2, 3$.

Δt	$E(\pi)_{M1}/E(\pi)_{M2}$	$E(\pi)_{M2}/E(\pi)_{M3}$
1.95E-03	1.60E+00	1.49E+00
9.77E-04	1.98E+00	5.57E-01
4.88E-04	2.11E+00	9.50E-01

Table 13: Ratios of spatial errors $E(\pi)_{M1}/E(\pi)_{M2}$ and $E(\pi)_{M2}/E(\pi)_{M3}$.

First Order Rusanov **Velocity**

Explicito-Cea	CFL VELVIS	Error M1	last dt	Error M2	last dt	Error M3	last dt	ErrorM1/ errorM2	ErrorM2/errorM3	Order	
Err t final	7,00E+00	8,42E-02	1,63E-02	3,94E-02	5,02E-03	2,00E-02	1,89E-03	2,14E+00	1,97E+00	1,095	0,980
Err t final	5,00E+00	8,42E-02	1,17E-02	3,95E-02	4,14E-03	2,00E-02		2,13E+00	1,97E+00	1,093	0,980
Err t final	4,00E+00	8,42E-02	9,32E-03	3,95E-02	3,31E-03	2,00E-02	1,08E-03	2,13E+00	1,97E+00	1,092	0,981
Err t final	3,00E+00	8,43E-02	7,00E-03	3,96E-02	2,48E-03	2,00E-02	8,09E-04	2,13E+00	1,97E+00	1,091	0,981
Err t final	2,00E+00	8,43E-02	4,67E-03	3,96E-02	1,66E-03	2,01E-02	5,39E-04	2,13E+00	1,97E+00	1,090	0,981
Err l2 tiempo	2,00E+00	4,68E-02	4,67E-03	2,14E-02	1,66E-03	1,01E-02	5,39E-04	2,18E+00	2,12E+00	1,127	1,087

Pressure

	CFL VELVIS	Error M1	Error M2	Error M3	ErrorM1/ errorM2	ErrorM2/errorM3	Order	
Err t final	7,00E+00	1,74E-01	7,56E-02	4,22E-02	2,30E+00	1,79E+00	1,199	0,843
Err t final	5,00E+00	1,78E-01	8,04E-02	4,36E-02	2,21E+00	1,84E+00	1,145	0,883
Err t final	4,00E+00	1,73E-01	8,73E-02	4,31E-02	1,98E+00	2,03E+00	0,986	1,018
Err t final	3,00E+00	1,73E-01	7,84E-02	4,39E-02	2,21E+00	1,78E+00	1,146	0,835
Err t final	2,00E+00	1,74E-01	8,12E-02	4,39E-02	2,15E+00	1,85E+00	1,103	0,888
Err l2 tiempo	2,00E+00	8,46E-02	3,94E-02	2,17E-02	2,15E+00	1,81E+00	1,104	0,856

Orden2 Cea-Vc convectivo

Explicito-CeaVC Viscosidad **Velocity**

	CFL VELVIS	Error M1	last dt	Error M2	last dt	Error M3	last dt	ErrorM1/errorM2	ErrorM2/errorM3	Order	
Err t final	7,00E+00	9,15E-02	1,63E-02	3,15E-02	5,81E-03	1,25E-02	1,89E-03	2,91E+00	2,52E+00	1,540	1,333
Err L2 tiempo	7,00E+00	7,39E-02		1,84E-02		7,10E-03		4,01E+00	2,60E+00	2,003	1,377

Pressure

	CFL VELVIS	Error M1	Error M2	Error M3	ErrorM1/errorM2	ErrorM2/errorM3	Order	
Err t final	7,00E+00	1,28E-01	3,09E-02	1,19E-02	4,139059963	2,59E+00	1,373	1,373
Err L2 tiempo	7,00E+00	6,54E-02	1,78E-02	6,56E-03	3,67E+00	2,71E+00	1,441	1,441

Orden2 convectivo + viscosidad

Explicito-Ce Viscosidad **Velocidad**

	CFL VELVIS	Error M1	Last dt	Error M2	DT VV tfinal-1	Error M3	Last dt	ErrorM1/errorM2	ErrorM2/errorM3	Order	
Err t final	7,00E+00	1,25E-01	1,69E-02	4,43E-02	5,83E-03	1,87E-02	1,89E-03	2,81E+00	2,89E+00	1,491	1,531
Err L2 tiempo	7,00E+00	8,46E-02		2,46E-02		9,75E-03		3,44E+00	2,52E+00	1,782	1,336
Err t final	2,00E+00	1,23E-01	4,80E-03	4,34E-02	1,67E-03	1,86E-02	5,41E-04	2,84E+00	2,34E+00	1,507	1,225
Err L2 tiempo	2,00E+00	6,47E-02		2,41E-02		9,71E-03		2,69E+00	2,48E+00	1,426	1,311

Pressure

	CFL VELVIS	Error M1	Error M2	Error M3	ErrorM1/errorM2	ErrorM2/errorM3	Order	
Err t final	7,00E+00	1,44E-01	5,42E-02	3,21E-02	2,66E+00	1,69E+00	1,409	0,754
Err L2 tiempo	7,00E+00	7,84E-02	2,69E-02	1,59E-02	2,91E+00	1,70E+00	1,542	0,762
Err t final	2,00E+00	1,37E-01	4,84E-02	3,07E-02	2,83E+00	1,58E+00	1,500	0,659
Err L2 tiempo	2,00E+00	6,66E-02	2,36E-02	9,71E-03	2,82E+00	2,43E+00	1,494	1,283

3. Flow around a cylinder

- 3D steady-state flow around a cylinder. It has been introduced in M. Schafer and S. Turek (1996) and employed in V. John (2002) as a benchmark problem.
- The computational domain consists of a solid cylinder surrounded by a rectangular channel in which the flow evolves.

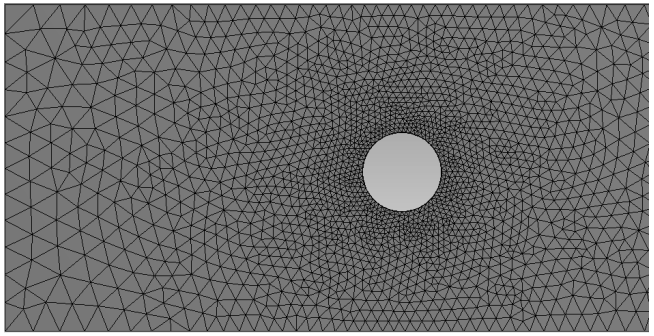

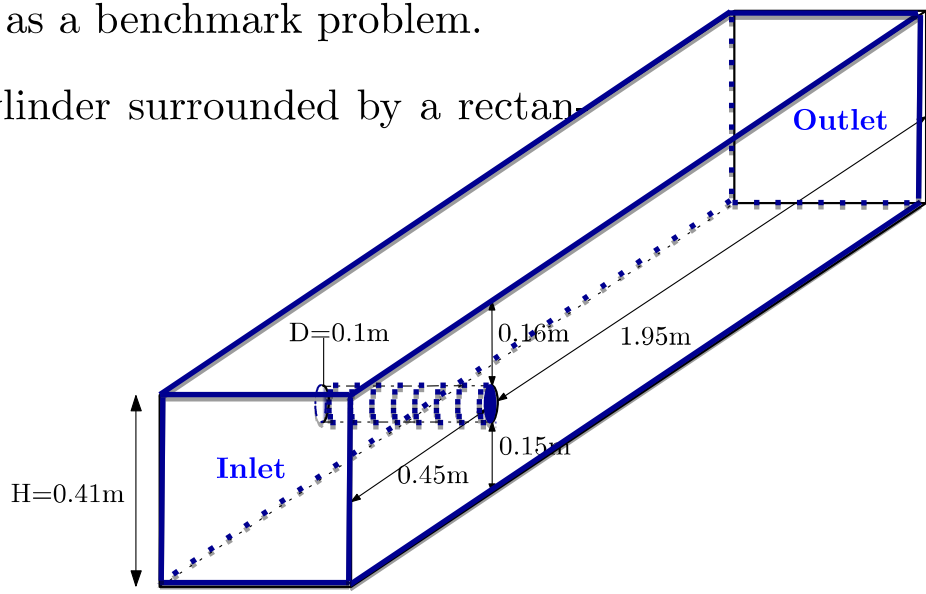

- The kinematic viscosity of the fluid is $\nu = 10^{-3} m^2/s$ and the inlet velocity has the form

$$\mathbf{u}(x, y, z, t) = \left(16Uyz(H - y)(H - z)/H^4, 0, 0\right)^t,$$

with $U = 0.45m/s$, $H = 0,41m$.

- Based on ν, the cylinder diameter and an estimate of $0.2m/s$ for the mean inflow velocity, the flow has a Reynolds number of 20.
- The mesh employed to obtain the numerical solution consists of 449 746 finite elements and 992 280 finite volumes.

Approximated w_x at $z=0$

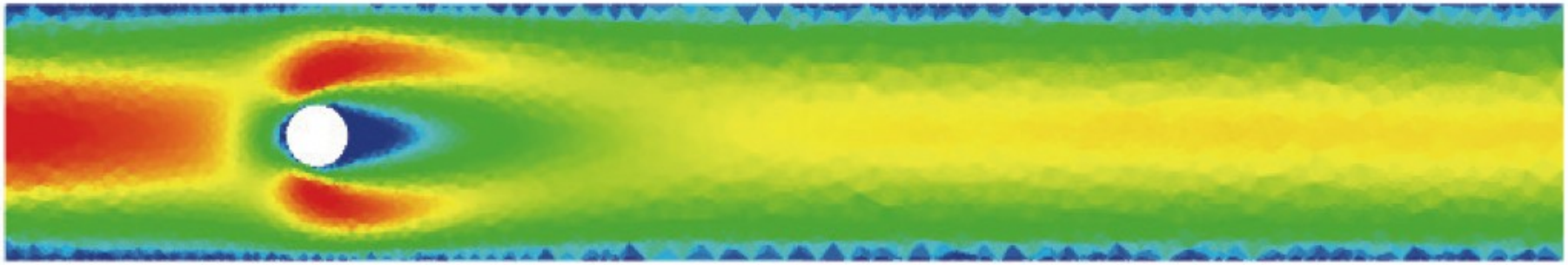

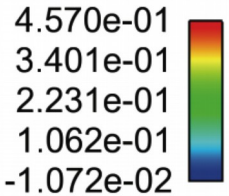

Approximated pressure at $z=0$

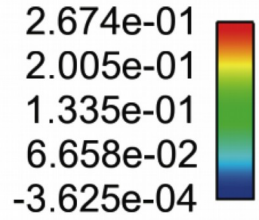

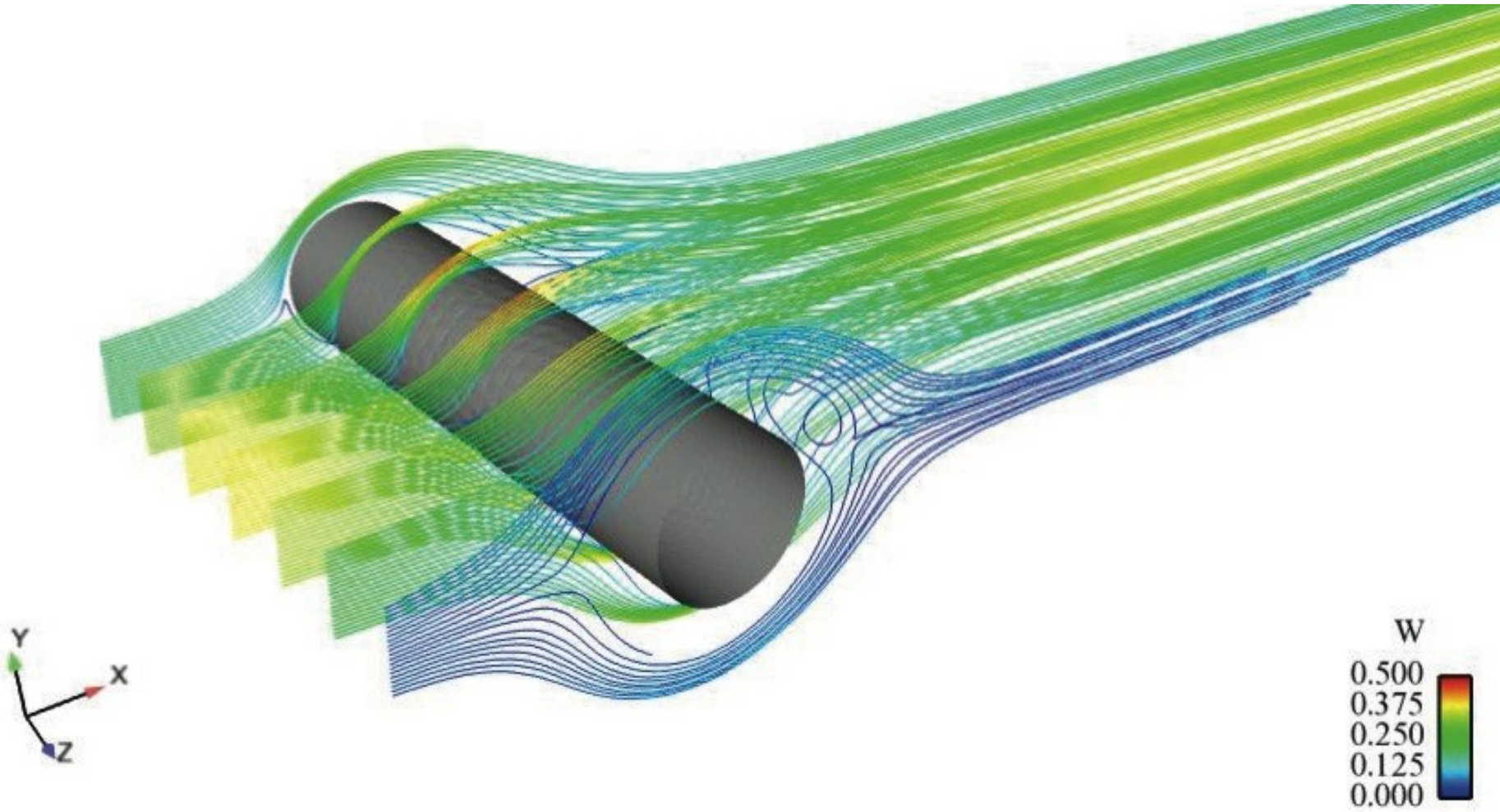

Streamlines

- The drag and lift coefficients:

$$c_d = \frac{500}{0.41} F_d, \;\; c_l = \frac{500}{0.41} F_l,$$

  - Drag force: F_d
  - Lift force: F_l

- The pressure difference Δp between the points $(0.45, 0.2, 0.205)$ and $(0.55, 0.2, 0.205)$.

Test case	Time iterations	CPU time	c_d (min,max) (6.05, 6.25)	c_l (min,max) (0.008, 0.01)	$D\pi$ (min,max) (0.165, 0.175)
T1 (1st Order)	1841	01:35:33	6.72	0.0053	0.1664
T2 (1st Order)	1745	01:36:20	6.79	0.0062	0.1656
T1 (2nd Order)	1841	01:35:33	6.33	0.0006	0.16373
T2 (2nd Order)	1745	01:36:20	6.34	0.0015	0.16350

Q-Scheme of van Leer (T1) and Rusanov (T2). 2nd Order Cea-VC method.

$$F_d = \int_S \left(\rho\nu \frac{\partial \mathbf{u}_\tau}{\partial \mathbf{n}_S} n_y - \pi n_x \right) \mathrm{dS}, \quad F_l = \int_S \left(-\rho\nu \frac{\partial \mathbf{u}_\tau}{\partial \mathbf{n}_S} n_x - \pi n_y \right) \mathrm{dS} \tag{58}$$

with $\mathbf{n}_S = (n_x, n_y, 0)^t$ the inward pointing unit normal with respect to Ω, S is the surface of the cylinder, and $\mathbf{n}_\tau = (n_y, -n_x, 0)^t$ is one of the tangential vectors, the other one being $(0, 0, 1)^t$. The computation of the integrals in (58) is done taking into account the relations

$$\frac{\partial \mathbf{u}_\tau}{\partial \mathbf{n}_S} n_y = \nabla u_1 \cdot \mathbf{n}_S, \tag{59}$$

$$\frac{\partial \mathbf{u}_\tau}{\partial \mathbf{n}_S} n_x = -\nabla u_2 \cdot \mathbf{n}_S, \tag{60}$$

obtained from the boundary condition $\mathbf{u}|_S = 0$. The approximate value of the the drag and lift forces is given by

$$(F_d^{n+1},\ F_l^{n+1})^t = \sum_{k=1}^{N_{BC}} \rho_k^{n+1} \nu_k^{n+1} \frac{area(\Gamma_k)}{|\widetilde{\boldsymbol{\eta}}_k \cdot \mathbf{V}_{kB}|} \mathbf{u}_{B_k}^{n+1} + area(\Gamma_k) \pi_k^{n+1} \widetilde{\boldsymbol{\eta}}_k, \tag{61}$$

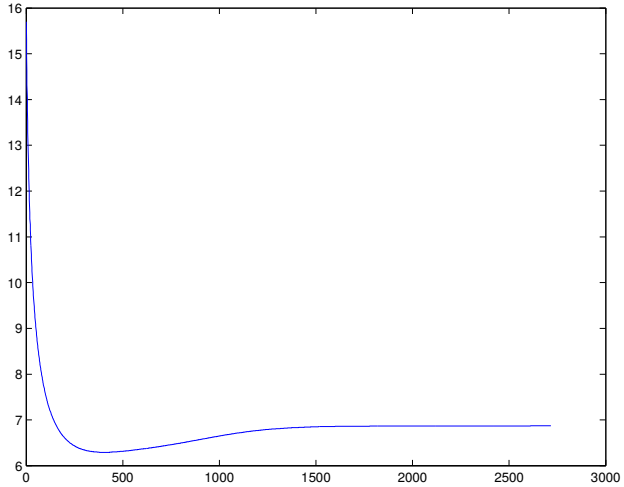

Drag coefficient

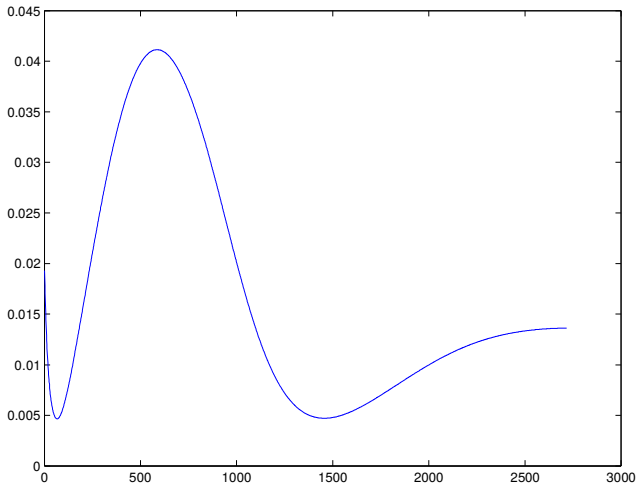

Lift coefficient

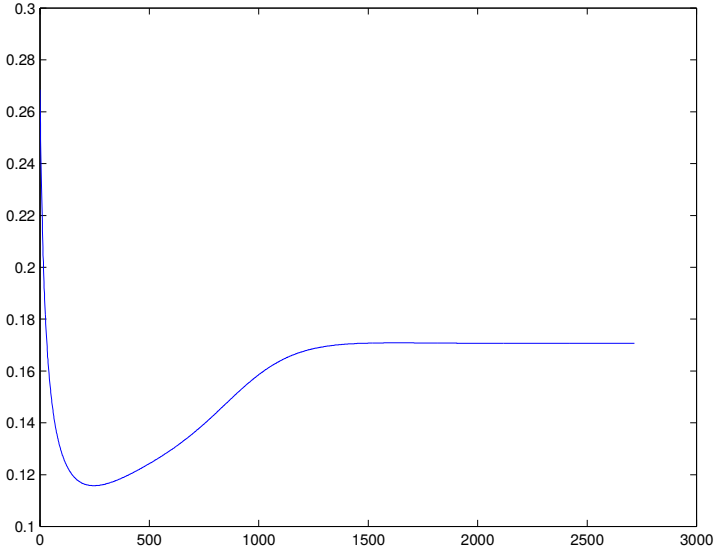

Pressure difference $\Delta\pi$ between points (0.45, 0.2, 0.205) and (0.55, 0.2, 0.205)

Low-Mach number equations with transport and energy equations

- The system of equations to be solved read

$$\frac{\partial \mathbf{w}}{\partial t} + \operatorname{div}(\mathcal{F}(\mathbf{w},\rho)) + \nabla\pi - \operatorname{div}(\tau) = \mathbf{f}(x,y,z,t),$$
$$\operatorname{div}\mathbf{w} = q,$$
$$\frac{\partial \overset{\triangle}{\mathbf{w}}}{\partial t} + \operatorname{div}(\overset{\triangle}{\mathcal{F}}(\overset{\triangle}{\mathbf{w}},\mathbf{w},\rho)) - \operatorname{div}\left(\rho\mathcal{D}\operatorname{grad}\frac{\overset{\triangle}{\mathbf{w}}}{\rho}\right) = \overset{\triangle}{\mathbf{f}}(x,y,z,t),$$

- The flux $\mathcal{F}$ and $\overset{\triangle}{\mathcal{F}}$ are given by:

$$\mathcal{F}_{\mathbf{i}}(\mathbf{w},\rho) = \frac{w_i}{\rho}\mathbf{w},\ i = 1,2,3.$$
$$\overset{\triangle}{\mathcal{F}}_{\mathbf{i}}(\overset{\triangle}{\mathbf{w}},\mathbf{w},\rho) = \frac{w_i}{\rho}\overset{\triangle}{\mathbf{w}},\ i = 1,...,N+1$$

Spatial dimension: $3 \longrightarrow \mathbf{w} = (w_1, w_2, w_3)^T$

Number of species: $N \longrightarrow \overset{\triangle}{\mathbf{w}}_i = \rho Y_i, i = 1,...,N$

Energy equation: $1 \longrightarrow \overset{\triangle}{\mathbf{w}}_{N+1} = \rho h,$

- We define a "generalized conservative variable", $\mathbf{w}^g$, as a combination of the previous conservative variables vector $\mathbf{w}$ and the new vector $\overset{\triangle}{\mathbf{w}}$, so that

$$\mathbf{w}^g = \begin{pmatrix} \mathbf{w} \\ \hline \overset{\triangle}{\mathbf{w}} \end{pmatrix}_{3+N+1}$$

- We define a "generalized conservative variable", $\mathcal{F}^g$

$$\mathcal{F}^{\mathbf{g}}(\mathbf{w}^g, \rho) = \frac{1}{\rho} \left(w_1 \mathbf{w}^g \;\middle|\; w_2 \mathbf{w}^g \;\middle|\; w_3 \mathbf{w}^g \right)_{(3+N+1)\times 3}$$

- More precisely, the expression for this tensor is as follows:

$$\mathcal{F}^{\mathbf{g}}(\mathbf{w}^g, \rho) = \frac{1}{\rho} \left(\begin{array}{ccc} w_1^2 & w_2 w_1 & w_3 w_1 \\ w_1 w_2 & w_2^2 & w_3 w_2 \\ w_1 w_3 & w_2 w_3 & w_3^2 \\ \hline w_1 \overset{\triangle}{w}_1 & w_2 \overset{\triangle}{w}_1 & w_3 \overset{\triangle}{w}_1 \\ \vdots & \vdots & \vdots \\ w_1 \overset{\triangle}{w}_N & w_2 \overset{\triangle}{w}_N & w_3 \overset{\triangle}{w}_N \\ \hline w_1 \overset{\triangle}{w}_{N+1} & w_2 \overset{\triangle}{w}_{N+1} & w_3 \overset{\triangle}{w}_{N+1} \end{array} \right)_{(3+N+1)\times 3}$$

Test with a transport equation: Gaussian sphere

- The computational domain of the flow, consisting in a cube of dimensions $\Omega = (-0.9, 0.9) \times (-0.9, 0.9) \times (-0.3, 0.3)$.
- The analytic solution:

$$\begin{aligned} \mathbf{u}(x,y,z,t) &= (-y, x, 0) \\ \pi(x,y,z,t) &= 1 \\ \rho(x,y,z,t) &= 1 \\ f(x,y,z,t) &= (-x, -y, 0) \end{aligned}$$

$$Y(x,y,t) = \left(\frac{\sigma_0}{\sqrt{\sigma_0^2 + 2\nu t}}\right)^3 \exp\left\{-\frac{\left(\overline{x(t)} + 0.25\right)^2 + \left(\overline{y(t)}\right)^2 + \left(\overline{z(t)}\right)^2}{2\left(\sigma_0^2 + 2\nu t\right)}\right\}$$

$$\begin{aligned} \overline{x(t)} &= x\cos t + y \sin t, \\ \overline{y(t)} &= -x \sin t + y \cos t, \\ \overline{z(t)} &= z \\ \sigma_0 &= 0.08, \end{aligned}$$

L. Saavedra (2012)

Conclusions

- The transport-diffusion stage is done by a time-explicit face finite volume discretization on a unstructured mesh, upwinded by classical approximate Riemann solvers.
- The projection stage consists of boundary-value problem for the Laplace operator that is solved by a standard finite element method.
- The use of face-type finite volumes facilitates the imposition of flux boundary conditions and leads to a staggered-like spatial discretization of velocity and pressure.
- In the case of steady-state problems a semi-implicit discretization is also proposed for the viscous term allowing for larger time steps than those needed for the fully explicit scheme.
- The method is applied to several different test problems allowing us to assess its accuracy. In general, first order is achieved, both in time and in space.
- Since the transport-diffusion stage is explicit in time and the matrix for the projection stage can be factorized only once because it is time independent, the overall method is cheap. Moreover, the transport-diffusion stage can be easily parallelized leading to a considerable improvement in the computational efficiency.

Obrigada!

elena.vazquez-cendon@usc.es